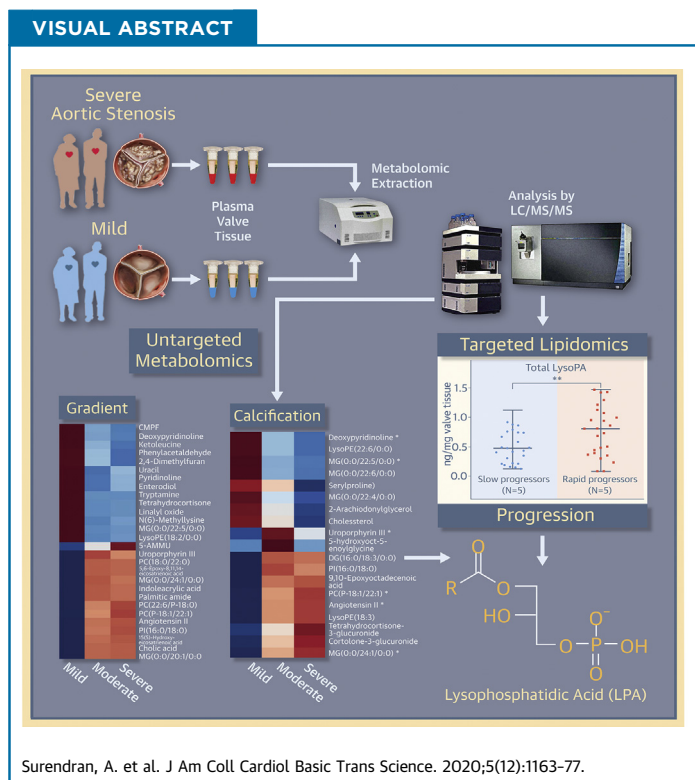**CLINICAL RESEARCH**

Metabolomic Signature of Human Aortic Valve Stenosis

Arun Surendran, BE, MBA,[a,b,c] Andrea Edel, PhD,[a,b] Mahesh Chandran, MSc,[c] Pascal Bogaert, MD,[a]
Pedram Hassan-Tash, MD,[b] Aneesh Kumar Asokan, PhD,[c] Brett Hiebert, BSc,[a] Zahra Solati, MSc,[a,b]
Shubhkarman Sandhawalia, MD,[a] Michael Raabe, MD,[d] Malek Kass, MD,[e] Ashish Shah, MD,[b,e]
Davinder S. Jassal, MD,[b,e] Abdul Jaleel, PhD,[c] Amir Ravandi, MD, PhD[a,b,e]

VISUAL ABSTRACT

Surendran, A. et al. J Am Coll Cardiol Basic Trans Science. 2020;5(12):1163–77.

HIGHLIGHTS

- This study is the first step towards the creation of a metabolomic map of calcified human aortic valves.
- The study highlights an independent association of LysoPA with CAVS severity.
- The study demonstrates that LysoPA levels are associated with faster CAVS progression rate.

From the [a]Cardiovascular Lipidomics Laboratory, St. Boniface Hospital, Albrechtsen Research Centre, Winnipeg, Manitoba,
Canada; [b]Department of Physiology and Pathophysiology, Rady Faculty of Health Sciences, University of Manitoba, Winnipeg,
Manitoba, Canada; [c]Mass Spectrometry and Proteomics Core Facility, Rajiv Gandhi Centre for Biotechnology, Kerala, India;
[d]Section of Cardiac Surgery, Rady Faculty of Health Sciences, University of Manitoba, Manitoba, Winnipeg, Canada; and the
[e]Section of Cardiology, Department of Medicine, Rady Faculty of Health Sciences, University of Manitoba, Winnipeg, Manitoba,
Canada.

ABBREVIATIONS AND ACRONYMS

AS = aortic stenosis

ATX = autotaxin

AV = aortic valve

AVA = aortic valve area

BAV = bicuspid aortic valve

CAVS = calcific aortic valve stenosis

CV = correlation of variation

Lp(a) = lipoprotein(a)

LysoPA = lysophosphatidic acid

LysoPC = lysophosphatidylcholine

LysoPE = lysophosphatidylethanolamine

MG = monoglyceride

MPG = mean pressure gradient

PC = phosphatidylcholine

QC = quality control

TAV = tricuspid aortic valve

Vmax = peak aortic jet velocity

SUMMARY

This study outlines the first step toward creating the metabolite atlas of human calcified aortic valves by identifying the expression of metabolites and metabolic pathways involved at various stages of calcific aortic valve stenosis progression. Untargeted analysis identified 72 metabolites and lipids that were significantly altered ($p < 0.01$) across different stages of disease progression. Of these metabolites and lipids, the levels of lysophosphatidic acid were shown to correlate with faster hemodynamic progression and could select patients at risk for faster progression rate. (J Am Coll Cardiol Basic Trans Science 2020;5:1163–77) © 2020 The Authors. Published by Elsevier on behalf of the American College of Cardiology Foundation. This is an open access article under the CC BY-NC-ND license (http://creativecommons.org/licenses/by-nc-nd/4.0/).

Calcific aortic valve stenosis (CAVS) is the most prevalent valvular disease reported in developed countries and is associated with significant morbidity and mortality ([1]). Thickening of the aortic valve (AV) leaflets by progressive fibrocalcific remodeling leads to narrowing of the valve orifice. This results in impaired leaflet motion and severe obstruction of the left ventricular outflow tract. The pathophysiology of CAVS is unknown, and there is no medical therapy to prevent or slow the natural progression of this disease. For patients with CAVS who have an indication for valve replacement, the only effective treatment options include either surgical AV replacement or transcatheter AV implantation. Although these interventions improve survival and relieve symptoms, they are costly and are associated with long-term morbidity and mortality ([2]). Therefore, there is a growing clinical need for novel pharmacological therapies to delay disease progression and provide better patient outcomes.

Advancements in "omics" research in the last decade, particularly genomics and proteomics, have allowed us to determine the changes within the genome and the proteome that occur during CAVS development. Recent Mendelian randomization studies have shown that variation in the *LPA* gene locus (rs10455872) mediated by lipoprotein(a) [Lp(a)] is involved in the development of CAVS ([3],[4]). In a recent study using both proteomics and transcriptomics approaches, Schlotter et al. ([5]) demonstrated that global transcriptional and protein expression signatures differed between various stages of CAVS progression. Unlike genes and proteins, which are predisposed to epigenetic changes and post-translational modifications, metabolites provide a true representation of cellular activity and therefore best characterize the molecular phenotype of the biological system (cells, tissues, or whole organism) ([6]). Metabolomics allows the unbiased identification and quantification of hundreds to thousands of small molecules and their interactions within a biological system at any given time point. In this context, metabolomics analysis of human stenotic valves characterized by varying degrees of disease severity can provide molecular-level information about the metabolites and metabolic pathways that are active at each stage of CAVS progression.

In this paper we present the largest and most comprehensive metabolomics study on stenotic human AVs. Given that CAVS progression and development is a multifactorial phenomenon, we conducted a detailed nontargeted and targeted metabolomics analysis to unmask the metabolic signatures in AV leaflets characterized by varying degrees of CAVS severity.

METHODS

Detailed descriptions of tissue procurement, AV morphology, sample preparation, sample grouping, tandem mass spectrometry conditions, compound identification, and statistics are provided in the Supplemental Methods. The complete untargeted metabolomics data have been deposited to the European Molecular Biology Laboratory-European

---

TABLE 1 Baseline Characteristics of the Study Population

| Clinical Parameter | Total (N = 106) | Stage of CAVS | | | p Value* |
		Mild (N = 15)	Moderate (N = 38)	Severe (N = 49)	
Age, yrs	70 (62,79)	72 (62,79)	75 (67,80)	67 (61,72)	0.101
Male	73 (68)	11 (73.3)	24 (63.2)	36 (73.5)	0.551
Height, cm	171 (163,176)	173 (160,177)	170 (165,175)	174 (165,178)	0.708
Weight, kg	84 (74,97)	77 (51,93)	84 (74,97)	91 (78,101)	0.049
Body surface area, m^2	1.97 ± 0.22	1.8 ± 0.3	2 ± 0.2	2 ± 0.2	0.029
Body mass index, kg/m^2	29.4 ± 5.6	25 ± 5.2	29.5 ± 5	30.6 ± 5.8	0.004
History of hypertension	68 (64)	8 (53.3)	29 (76.3)	34 (69.4)	0.577
Smoking history	56 (53)	5 (33.3)	28 (73.7)	22 (44.9)	0.005
Current	10 (9)	0	5 (13.1)	5 (10.2)	
Previous	43 (41)	5 (33.3)	22 (57.8)	16 (32.6)	
Never	44 (42)	7 (46.7)	8 (21)	26 (53)	
Medication					
Antihypertensive treatment	65 (61)	8 (53.3)	24 (63.2)	30 (61.2)	0.872
ACE inhibitors	31 (29)	6 (40)	10 (26.3)	14 (28.6)	0.541
ARBs	11 (10)	2 (13.3)	4 (10.5)	4 (8.2)	0.807
Statins	59 (55)	4 (26.7)	21 (55.3)	32 (65.3)	0.031
Laboratory data					
LDL cholesterol, mmol/l	2.5 (1.7,3.2)	2.6 (1.9,3.6)	2.5 (2.0,3.5)	2.5 (1.7,3.2)	0.714
HDL cholesterol, mmol/l	1.3 (1.0,1.6)	1.3 (1.0,1.8)	1.3 (1.0,1.5)	1.3 (1.0,1.6)	0.477
Triglycerides, mmol/l	1.4 (0.9,1.7)	1.1 (0.8,1.6)	1.4 (0.9,1.7)	1.4 (1.0,1.8)	0.401
Random glucose, mmol/l	6.4 (5.4,8.3)	6.5 (5.6,7.5)	6.2 (5.5,9.7)	6.5 (5.2,8.3)	0.903
Creatinine (μmol/l)	83 (71,102)	82 (59,91)	83 (70,99)	82 (71,109)	0.722
Doppler echocardiographic data					
Bicuspid aortic valve	29 (28)	5 (33.3)	10 (26.3)	14 (28.6)	0.841
Aortic valve calcification score					
1	10 (10)	8 (53.3)	0	1 (2)	
2	28 (27)	2 (13.3)	14 (36.8)	10 (20.4)	
3	39 (38)	3 (20)	16 (42.1)	20 (40.8)	
4	18 (18)	0	6 (15.7)	12 (24.4)	
5	7 (7)	1 (6.67)	1 (2.63)	5 (10.2)	
Peak aortic jet velocity, m/s	4.0 (3.6,4.5)	2.3 (1.6,2.7)	3.8 (3.5,3.9)	4.5 (4.2,5.1)	<0.001
Peak pressure gradient, mm Hg	65 (50,81)	18 (14,27)	57 (48,61)	82 (73,103)	<0.001
Mean pressure gradient, mm Hg	39 (30,50)	11 (8,15)	34 (29,37)	51 (46,65)	<0.001
Aortic valve area, cm^2	0.9 (0.7,1.0)	1.7 (1.2,2.3)	0.9 (0.8,1.0)	0.8 (0.6,0.9)	<0.001
Indexed aortic valve area, cm^2/m^2	0.4 (0.4,0.5)	0.9 (0.7,1.2)	0.5 (0.4,0.5)	0.4 (0.3,0.5)	<0.001
Left ventricular mass index, g/m^2	128 (102,149)	166 (141,188)	114 (89,134)	127 (103,145)	0.001
Left ventricular ejection fraction, %	60 (55,60)	50 (40,60)	60 (55,60)	60 (60,60)	0.030

Values are median (25th, 75th percentiles), n (%), or mean ± SD. The chi-square test was used for categorical variables, and the Kruskal-Wallis test or 1-way analysis of variance was used for continuous variables to assess for statistical significance between sample groups as applicable based on data distribution. *The p values were obtained after subgroup comparison (mild, moderate, and severe groups) based on mean pressure gradient.

ACE = angiotensin-converting enzyme; ARB = angiotensin II receptor blocker; HDL = high-density lipoprotein; LDL = low-density lipoprotein.

Bioinformatic Institute MetaboLights database with the identifier MTBLS1267 (7). The study was approved by the ethics committee of both the University of Manitoba and the St. Boniface Hospital research ethics boards.
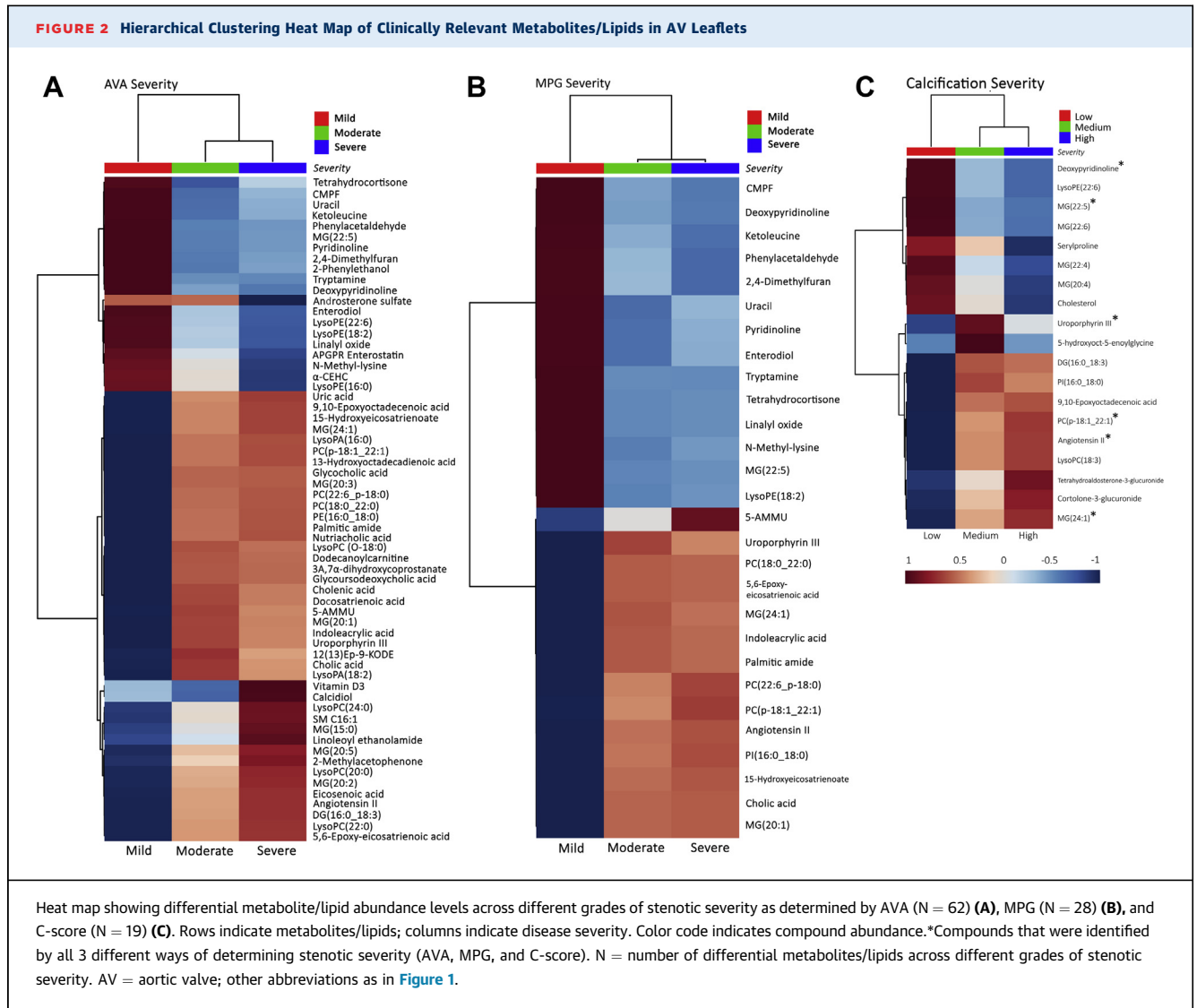
RESULTS

BASELINE CHARACTERISTICS. Baseline clinical and echocardiographic characteristics are listed in **Table 1**. Detailed patient information, stages of disease, and other clinical parameters are summarized in Supplemental Tables S2 and S3. A total of 106 patients (median age 70 years; 33 women and 73 men) participated in the study. A large proportion of the study population had a pre-existing history of hypertension (64%) and smoking (53%). Patients in the mild category were comparable to those in the severe category with respect to baseline clinical characteristics, including age, sex, and lipid profile measurements (**Table 1,** Supplemental Tables S2 and S3). However, clinically important hemodynamic measures, including peak aortic jet velocity (Vmax), mean pressure gradient (MPG), and aortic valve area (AVA),
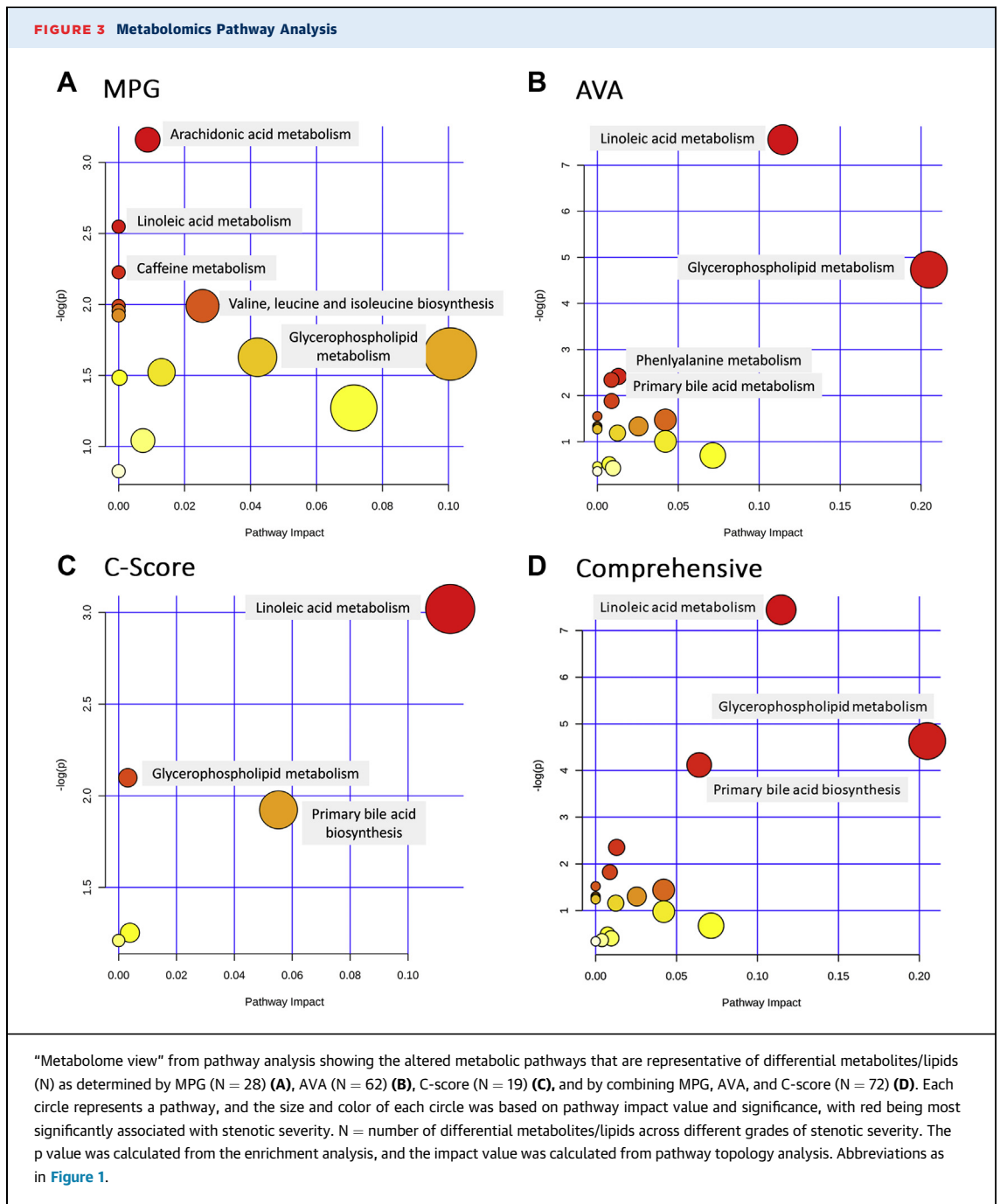
FIGURE 1   Metabolite Atlas of CAVS
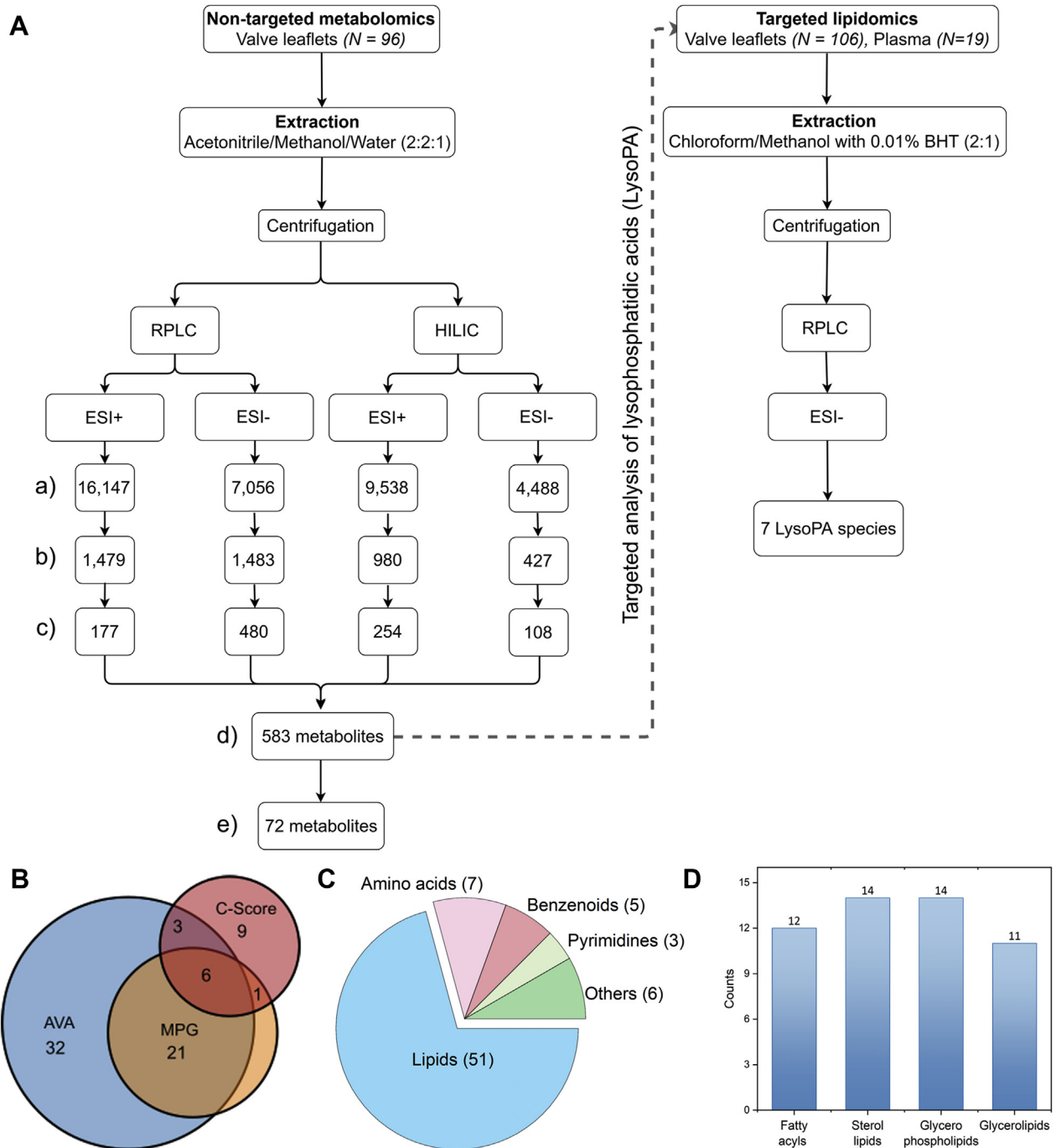
(A) Summary of metabolomics workflow depicting the observed number of molecular entities (features) with a unique m/z and retention time obtained from each mode of chromatographic separation **(a)**, features with correlation of variation (CV) <30% in quality control (QC) samples **(b)**, putatively annotated compounds in the Human Metabolome Database **(c)**, unique metabolites after removal of duplicates **(d)**, and differential metabolites (i.e., CV among QC samples <30%; p < 0.01, and fold change >2) **(e)** across different grades (mild, moderate, and severe) of calcific aortic valve stenosis (CAVS) severity. **(B)** Number of differential metabolites that were shared or unique based on different methods of determining the severity of aortic stenosis: mean pressure gradient (MPG), aortic valve area (AVA), and aortic valve calcification score (C-score). **(C)** Classification of differential metabolites (N = 72) according to their chemical class. **(D)** Subclassification hierarchy of identified lipids (N = 51). BHT = butylated hydroxytoluene; ESI = electrospray ionization; HILIC = hydrophilic interaction liquid chromatography; LysoPA = lysophosphatidic acid; RPLC = reverse phase liquid chromatography.

FIGURE 2 Hierarchical Clustering Heat Map of Clinically Relevant Metabolites/Lipids in AV Leaflets

Heat map showing differential metabolite/lipid abundance levels across different grades of stenotic severity as determined by AVA (N = 62) **(A)**, MPG (N = 28) **(B),** and C-score (N = 19) **(C)**. Rows indicate metabolites/lipids; columns indicate disease severity. Color code indicates compound abundance.*Compounds that were identified by all 3 different ways of determining stenotic severity (AVA, MPG, and C-score). N = number of differential metabolites/lipids across different grades of stenotic severity. AV = aortic valve; other abbreviations as in **Figure 1**.

differed significantly (p < 0.05) between various disease stages.

METABOLIC SIGNATURES THAT ASSOCIATE WITH CAVS SEVERITY. A summary of the metabolomics workflow is depicted in **Figure 1A**. From the 583 putatively identified metabolites (coefficient of variation [CV] of quality control [QC] <30%), those that exhibited abundance difference across different disease stages (differential metabolites) were further filtered out according to the following criteria: fold change >2 and analysis of variance p < 0.01. Among mild, moderate, and severe stages, 28 differential metabolites were identified via classification based on MPG, 62 were identified via classification based on AVA, and 19 were identified via classification based on AV calcification score (C-score). The retention times and mass spectral

patterns (mass-to-charge ratio [m/z]) of these significantly altered metabolites, including p value, q value (adjusted p value using False Discovery Rate), and fold change, are provided in Supplemental Tables S4 to S6. The proportional Venn diagram shows the number of metabolites that were shared or were unique within these 3 methods for determining CAVS severity (**Figure 1B**). With the exception of 1 metabolite, all differential metabolites that were identified via MPG classification overlap with those identified via AVA classification. However, AVA classification within the same cohort resulted in identification of far more differential metabolites (N = 62) compared to MPG classification (N = 28). Overall, 72 significantly altered metabolites were identified across 3 stages of CAVS severity (i.e., CV among QC samples <30%; p < 0.01, and fold change >2).

FIGURE 3   Metabolomics Pathway Analysis

"Metabolome view" from pathway analysis showing the altered metabolic pathways that are representative of differential metabolites/lipids (N) as determined by MPG (N = 28) **(A)**, AVA (N = 62) **(B)**, C-score (N = 19) **(C)**, and by combining MPG, AVA, and C-score (N = 72) **(D)**. Each circle represents a pathway, and the size and color of each circle was based on pathway impact value and significance, with red being most significantly associated with stenotic severity. N = number of differential metabolites/lipids across different grades of stenotic severity. The p value was calculated from the enrichment analysis, and the impact value was calculated from pathway topology analysis. Abbreviations as in **Figure 1**.

Among these metabolites, 23 compounds were further validated using the in-house theoretical fragmentation database (Supplemental Table S7). Lipids (N = 51) formed the largest pool of these differential metabolites, followed by amino acids, benzenoids, pyrimidines, and others (**Figure 1C**). Subclassification hierarchy organizes this lipid pool into 4 main lipid categories: fatty acyls, sterol lipids, glycerophospholipids, and glycerolipids (**Figure 1D**).

To visualize the similarities and differences in metabolic profile between different stages of CAVS, the relative average normalized intensities of these putatively identified differential metabolites and lipids were plotted as a heat map using MetaboAnalyst 4.0, an open source R-package for metabolomics data analysis (**Figure 2**). From the hierarchical heat map, it was evident that the mild stage was distinct from the moderate and severe stages.

FIGURE 4 Metabolite-Clinical Parameter and Metabolite-Metabolite Correlation Analysis
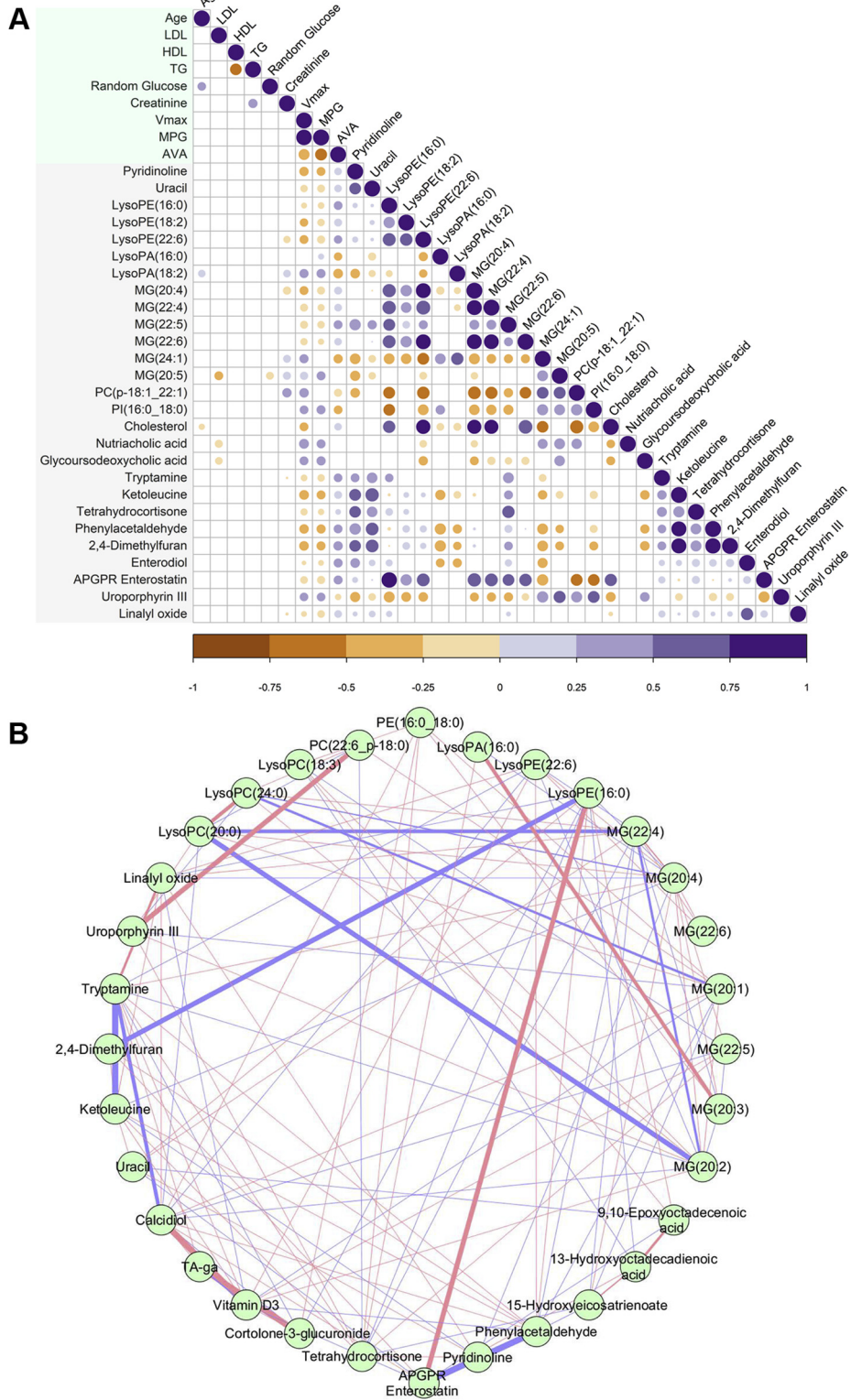
Noticeably, of the 72 differential metabolites and lipids, 6 [deoxypyridinoline, MG(22:5), MG(24:1), PC(p-18:1_22:1), uroporphyrin III, and angiotensin II] were consistently identified across all 3 aortic stenosis (AS) classifications (AVA, MPG, and C-score) (**Figures 2A to 2C**).

METABOLIC PATHWAYS INVOLVED IN DISEASE PROGRESSION. To obtain information on the metabolic pathways that are active in disease progression, a metabolomics pathway analysis was performed utilizing MetaboAnalyst using the KEGG pathway database (8). Separate pathway plots representing 28 differential metabolites and lipids based on MPG, 62 differential metabolites and lipids based on AVA, 19 differential metabolites and lipids based on the C-score, and a comprehensive pathway plot representing 72 differential metabolites and lipids were summarized in **Figures 3A to 3D**, respectively. Based on impact score and p value, the top 3 significantly altered metabolomics pathways that were associated with CAVS severity were the pathways involved in lipid metabolism and biosynthesis: glycerophospholipid metabolism, linoleic acid metabolism, and bile acid biosynthesis. We also evaluated whether the tissue metabolome of patients with bicuspid aortic valve (BAV) stenosis differs from that of patients with tricuspid aortic valve (TAV) stenosis. Our untargeted approach showed that there were no alterations in metabolome between these 2 populations (Supplemental Figure S1).

CORRELATION BETWEEN DIFFERENTIAL LIPIDS AND CLINICAL INDICATORS OF CAVS SEVERITY. To investigate the association between differential metabolites/lipids and biochemical indicators of CAVS severity, correlations were calculated using the R statistical package (R Foundation for Statistical Computing, Vienna, Austria) corrplot using Spearman correlation. From the resultant correlogram (**Figure 4A**), it was evident that the associations between important biochemical markers (age,
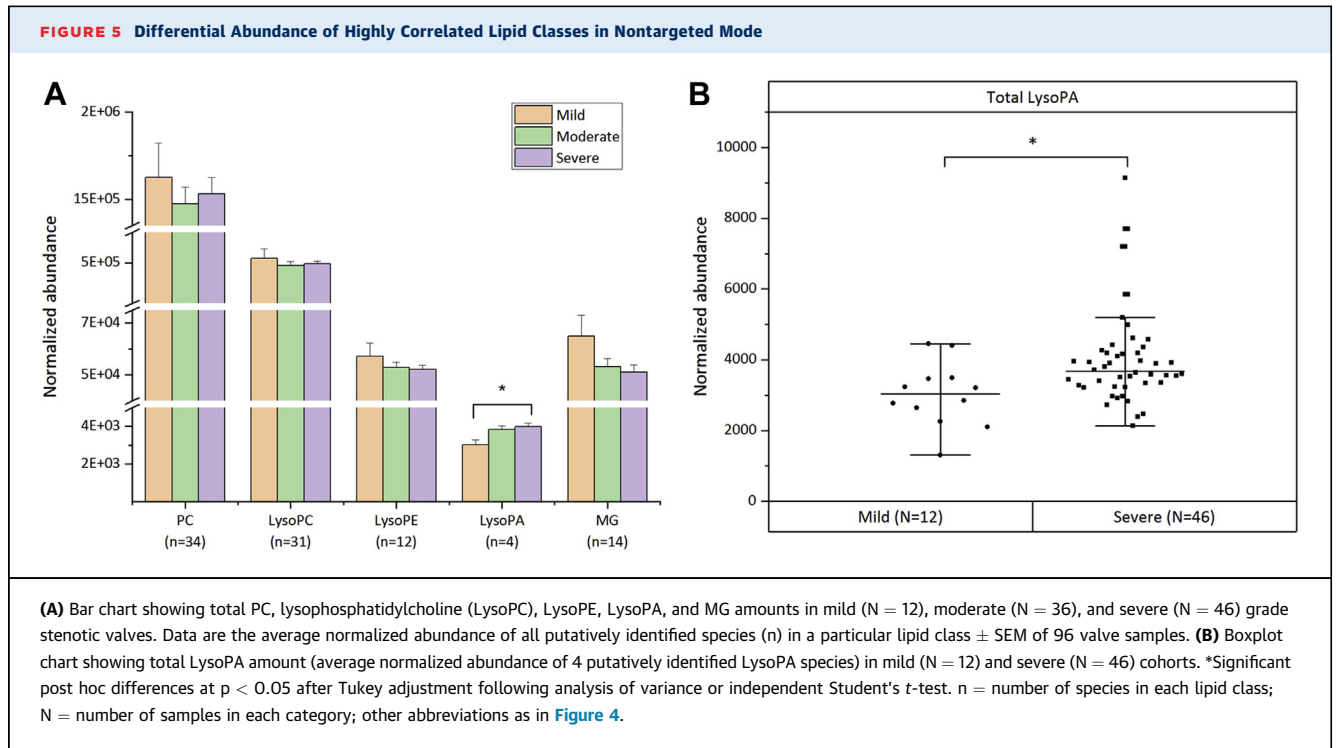
low-density lipoprotein, high-density lipoprotein, triglycerides, random glucose, and creatinine) and differential metabolites/lipids were comparably weak, whereas the associations between hemodynamic indicators of CAVS severity (Vmax, MPG, and AVA) and differential metabolites/lipids were significant (p < 0.05). Among the various related lipid classes, lysophosphatidylethanolamine (LysoPE) and monoglyceride (MG) species exhibited significant negative correlation with MPG and Vmax, whereas lysophosphatidic acid (LysoPA) species showed significant positive correlation with MPG and Vmax. The same lipids exhibited inverse correlations with AVA. Considering the well-known inverse relationship between MPG and AVA, this hints at a possible biochemical relationship among LysoPE, MG, and LysoPA species due to the action of an upstream enzyme(s). Notably, pyridinoline, a specific marker of bone degradation, showed significant negative correlation with MPG and significant positive correlation with AVA. Also noteworthy is the bile acid metabolite glycoursodeoxycholic acid, which exhibited significant positive correlation with MPG and Vmax.

ASSOCIATION NETWORK OF DIFFERENTIAL METABOLITES AND LIPIDS. As metabolites and lipids act in a coordinated manner and not in isolation, an association between them could provide valuable insights into the underlying disease process (9). To visualize this association, a correlation network plot was constructed using the Cytoscape software version 3.7.1 (National Institute of General Medical Sciences, Bethesda, Maryland) (**Figure 4B**). The resultant highly correlated metabolite set (32/72 metabolites/lipids) was dominated mainly by phosphatidylcholine (PC), lysophosphatidylcholine (LysoPC), LysoPE, LysoPA, and MG species. They were either positively or negatively correlated to each other. To further explore the role of these related lipid classes in disease progression, we determined the total abundance of these lipid classes across

---

FIGURE 4   Continued

(A) Differential metabolites/lipids were correlated with clinical parameters. Positive correlations are displayed in **purple** and negative correlations in **orange**. Color intensity and size of the circle are proportional to the correlation coefficients (Spearman correlation). In this correlogram, correlations with p > 0.05 are considered insignificant and are left blank. Only those metabolites or lipids (27) having more than 1 significant correlation (p < 0.05) with any of the 3 hemodynamic parameters—peak aortic jet velocity (Vmax), MPG, and AVA—were used to construct the correlogram. **(B)** Network plot highlighting the highly correlated metabolites/lipids. The nodes represent compounds, and the edges represent biochemical reactions. The thickness of the edges represents the strength of the correlations. The connections between the nodes were established by Pearson correlation ($|r_p| > 0.8$). Positive correlations are displayed in **pink** and negative correlations in **violet**. APGR = Ala-Pro-Gly-Pro-Arg; HDL = high-density lipoprotein; LDL = low-density lipoprotein; LysoPA = lysophosphatidic acid; LysoPE = lysophosphatidylethanolamine; MG = monoglyceride; PC = phosphatidylcholine; PI = Phosphatidylinositol; TA-ga = Tetrahydroaldosterone-3-glucuronide; TG = triglyceride; other abbreviations as in **Figure 1**.

FIGURE 5   Differential Abundance of Highly Correlated Lipid Classes in Nontargeted Mode

(A) Bar chart showing total PC, lysophosphatidylcholine (LysoPC), LysoPE, LysoPA, and MG amounts in mild (N = 12), moderate (N = 36), and severe (N = 46) grade stenotic valves. Data are the average normalized abundance of all putatively identified species (n) in a particular lipid class ± SEM of 96 valve samples. **(B)** Boxplot chart showing total LysoPA amount (average normalized abundance of 4 putatively identified LysoPA species) in mild (N = 12) and severe (N = 46) cohorts. *Significant post hoc differences at p < 0.05 after Tukey adjustment following analysis of variance or independent Student's *t*-test. n = number of species in each lipid class; N = number of samples in each category; other abbreviations as in **Figure 4**.

different disease stages stratified by MPG (**Figure 5A**). The final curated metabolite set containing 583 putatively annotated metabolites and lipids (CV QC <30%) included 34 PC species, 31 LysoPC species, 12 LysoPE species, 4 LysoPA species, and 14 MG species (Supplemental Table S9). Among these related lipid classes, only the total amount of LysoPA species differed significantly (p = 0.046) between the various disease stages (**Figures 5A and 5B**). This finding shows a strong association of LysoPAs to CAVS severity.
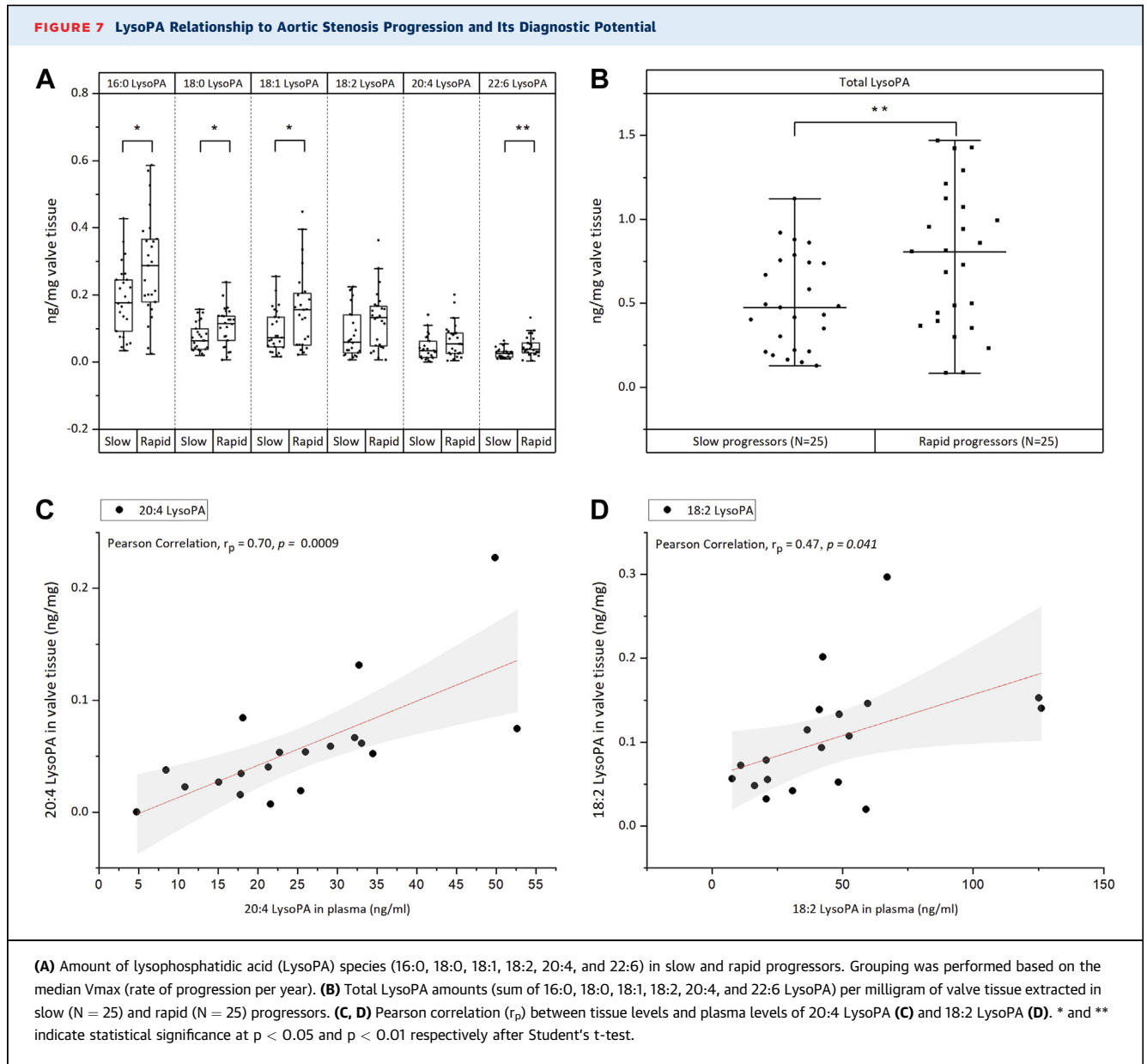
LysoPAs IN STENOTIC AV LEAFLETS. To further validate and confirm the results from nontargeted metabolomics analysis on the observed significant association of LysoPAs with CAVS severity, we performed a targeted (scheduled multiple reaction monitoring) analysis of LysoPA species using an LC-ESI-MS/MS platform as previously described (10). In brief, we identified and quantitated the 7 most common LysoPA species in 106 AV tissues. The patients were grouped into either low- or high-gradient groups centered on the median (25th, 75th percentiles) MPG value [39 (29.7, 49.7) mm Hg] of the cohort. The amount of individual LysoPA species (16:0, 18:0, 18:1, 18:2, 20:4, and 22:6) as well as total LysoPA amount were found to be significantly (p < 0.05) greater in the high-gradient group compared to the low-gradient group (**Figures 6A and 6B**). In addition, 16:0 LysoPA was found to be the most abundant species in the

stenotic AV leaflets (**Figure 6A**). Likewise, we compared the LysoPA levels across large and small AVA groups categorized according to the median (25th, 75th percentiles) AVA value of the cohort [0.9 (0.7,1.0) cm²]. In line with the classification based on MPG, there was a general trend of increased LysoPA levels in the small AVA group compared to the large AVA group (**Figures 6C and 6D**). Based on C-score classification, the total LysoPA amount as well as the individual amount of LysoPA species (18:0, 18:1, 18:2, 20:4) differed significantly (p < 0.05) between patients with C-score = 1 and C-score = 5 (**Figures 6E and 6F**). We also investigated the relationship of LysoPA levels with known risk factors of CAVS, including age, sex, lipid profile, glucose level, creatinine level, smoking habit, prevalence of hypertension, and presence of BAV. Our results show that total LysoPA amount is independent of these traditional risk factors (Supplemental Figures S2 and S3, and Supplemental Tables S10-A and S10-B).

LysoPAs ACCELERATE THE PROGRESSION OF CAVS SEVERITY. We retrospectively investigated in our cohort whether the increased levels of LysoPAs observed in severely stenotic AVs would translate into faster progression of AV calcium burden. In our entire cohort, a total of 50 patients had at least 2 previous echocardiography reports measuring peak Vmax before surgery (Supplemental Table S11). The

FIGURE 6   LysoPA Species in Valve Leaflets by Targeted LC/MS/MS Analysis
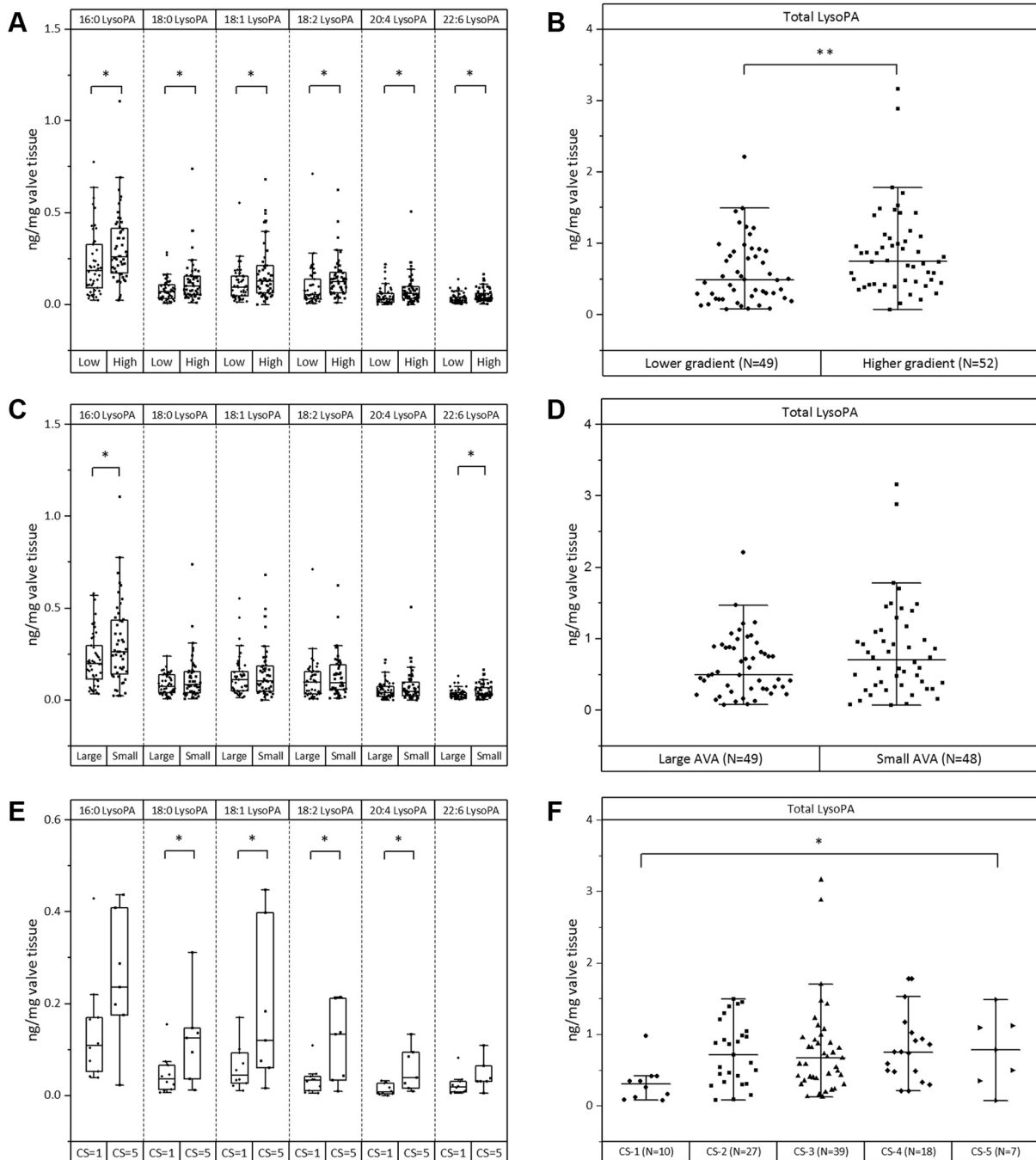
(A) Amount of LysoPA species (16:0, 18:0, 18:1, 18:2, 20:4 and 22:6) in low-gradient (Low) and high-gradient (High) groups. Grouping was performed based on median MPG of the cohort. (B) Total LysoPA amounts (sum of 16:0, 18:0, 18:1, 18:2, 20:4, and 22:6 LysoPA) per milligram of valve tissue extracted in Low (N = 49) and High (N = 52) groups. (C) Amount of LysoPA species (16:0, 18:0, 18:1, 18:2, 20:4, and 22:6) in large AVA (Large) and small AVA (Small) groups. Grouping was performed based on median AVA of the cohort. (D) Total LysoPA amounts (sum of 16:0, 18:0, 18:1, 18:2, 20:4, and 22:6 LysoPA) per milligram of valve tissue extracted in Large (N = 49) and Small (N = 48) groups. (E) Amount of LysoPA species (16:0, 18:0, 18:1, 18:2, 20:4, and 22:6) in 2 extremes of the 5-grade scoring system for valve calcification (C-score = 1 and C-score = 5). (F) Total LysoPA amounts (sum of 16:0, 18:0, 18:1, 18:2, 20:4, and 22:6 LysoPA) per milligram of valve tissue extracted in different grades of valve calcification. Statistical significance at *p < 0.05 and **p < 0.01 after Tukey adjustment following analysis of variance or independent Student's *t*-test. CS = calcification score; LC-ESI-MS/MS = liquid chromatography electrospray ionization tandem mass spectrometry; other abbreviations as in **Figures 1 and 4.**

FIGURE 7 LysoPA Relationship to Aortic Stenosis Progression and Its Diagnostic Potential

(A) Amount of lysophosphatidic acid (LysoPA) species (16:0, 18:0, 18:1, 18:2, 20:4, and 22:6) in slow and rapid progressors. Grouping was performed based on the median Vmax (rate of progression per year). (B) Total LysoPA amounts (sum of 16:0, 18:0, 18:1, 18:2, 20:4, and 22:6 LysoPA) per milligram of valve tissue extracted in slow (N = 25) and rapid (N = 25) progressors. (C, D) Pearson correlation (r_p) between tissue levels and plasma levels of 20:4 LysoPA (C) and 18:2 LysoPA (D). * and ** indicate statistical significance at $p < 0.05$ and $p < 0.01$ respectively after Student's t-test.

median rate of increase in aortic jet velocity in this subgroup was 0.33 (m/s)/year [range 0.03 to 2.42 (m/s)/year]. Patients with an increase in Vmax ≥0.33 (m/s)/year were considered as rapid progressors (N = 25) and others as slow progressors (N = 25). The total LysoPA amount was significantly higher (p = 0.008) in rapid progressors compared to slow progressors (**Figure 7B**). The same trend was also observed for all individual LysoPA species (**Figure 7A**).

DIAGNOSTIC POTENTIAL OF LysoPAs FOUND IN TISSUES. Compared to body fluid metabolome, tissue metabolome can provide metabolic signatures that directly associate with severity of AS. However, only circulating metabolites could serve as

biomarkers for clinical diagnosis. Therefore, we also explored the diagnostic potentials of these LysoPA species by quantifying them in a small cohort of plasma samples (N = 19) (Supplemental Table S12). Interestingly, Pearson correlation analysis (Supplemental Table S13) showed that the plasma amounts of 2 LysoPA species, 20:4 (r_p = 0.7; p = 0.0009) and 18:2 LysoPA (r_p = 0.47; p = 0.041), have significant correlation with their amounts in tissues (**Figures 7C and 7D**). If validated in an independent large cohort, this finding offers the potential to select patients who have a greater need for valve replacement by looking at the level of LysoPA in their blood plasma.

FIGURE 8 **Metabolomics of CAVS in Humans**
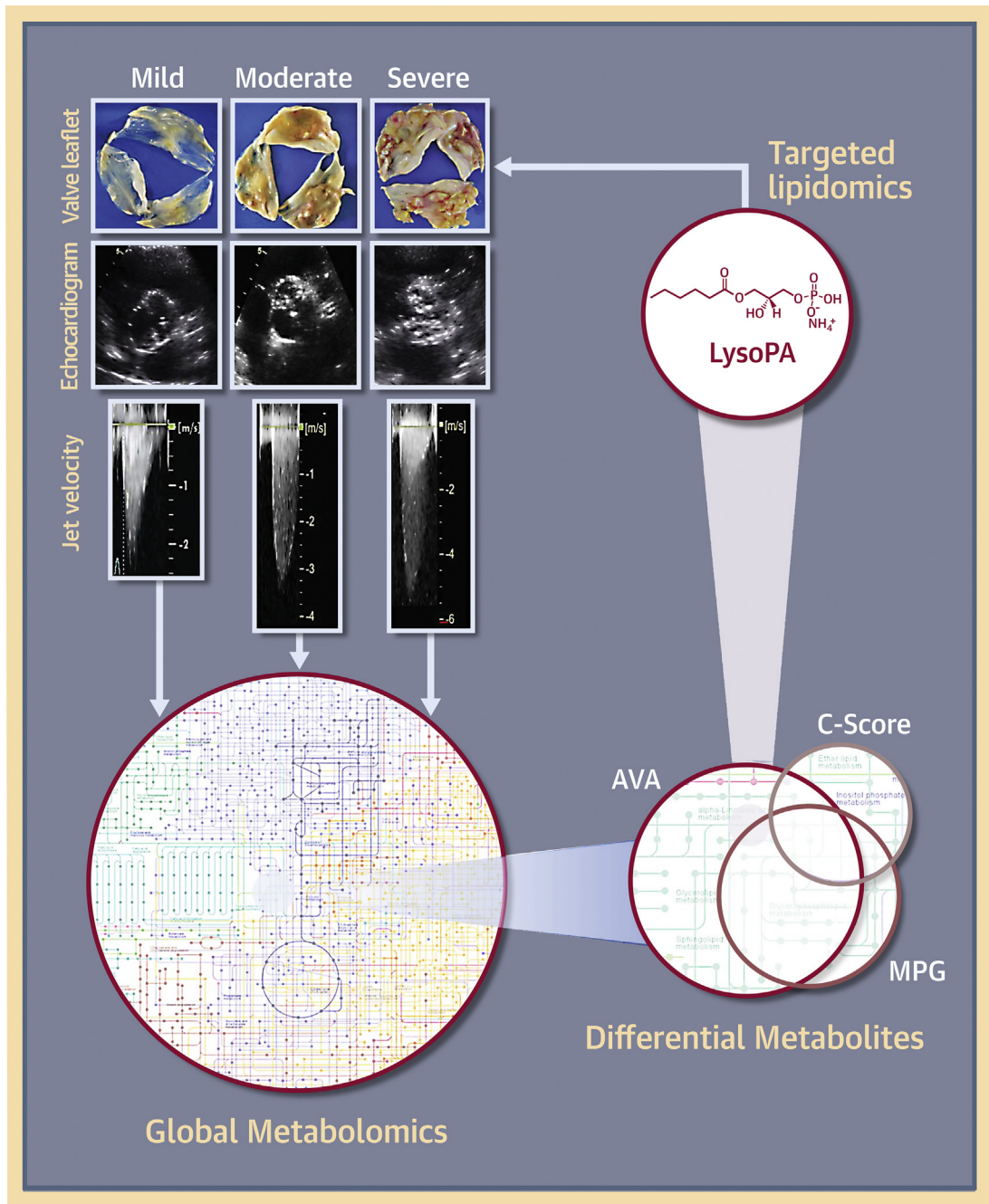
Schematic diagram showing representative images of explanted aortic valve leaflets, echocardiograms, and jet velocities in patients with varying degrees (mild, moderate, and severe) of calcific aortic valve stenosis (CAVS) severity and subsequent metabolomics workflow. Abbreviations as in **Figures 1 and 4**.

DISCUSSION

Complete knowledge of the disturbances of metabolites in any tissue allows for an unbiased look at the molecular processes that result in disease initiation and progression (11). Current metabolomics platforms can determine the changes in thousands of metabolites in tissue samples, allowing us to draw a

comprehensive atlas of metabolites that are altered in disease processes. Given the poorly understood disease mechanism in CAVS, we used nontargeted metabolomics, an unbiased, hypothesis-generating approach, to better understand the metabolic factors that result in the development and progression of this disease in humans. We further confirmed our findings by using a targeted lipidomics approach.

The primary goal of this study was to establish the metabolome map of human CAVS by uncovering the metabolic differences in human stenotic AVs characterized by varying degrees of disease severity (Figure 8). From the detected 37,229 metabolite features belonging to various metabolite and lipid classes, our results provide compelling evidence about an independent association of LysoPAs with CAVS severity. In comparison with other related lipid classes (PC, LysoPC, LysoPE, and MG) that exhibited strong association with CAVS severity, only the level of LysoPA differed significantly (p = 0.046) between mild and severe AS. The goal of this untargeted metabolomics approach was to highlight specific metabolomic pathways that can contribute to pathophysiology. Although the methods described here are designed for aqueous-soluble metabolites, some polar lipids may be extracted as well; LysoPA is 1 example. It is imperative to state that data from moderately polar or nonpolar lipids (diacylglyceride, PC, cholesterol ester, triglyceride, etc.) may only be partially extracted and/or resolubilized; therefore, the integrity of these measurements must be considered in the context of the extraction and analysis method used here. Ultimately, these changes must be confirmed using a targeted approach, as in the case for LysoPA, in which we utilized a dedicated extraction and analytical system. We demonstrated for the first time that elevated LysoPA levels were associated with faster CAVS progression rate. Our results showed that total valvular LysoPA levels were significantly higher in patients with faster progression rates than in those with slower progression rates.

LysoPA is a simple bioactive phospholipid that exerts pleiotropic biological effects under diverse physiological and pathophysiological conditions. It binds to diverse G protein–coupled receptors and invokes multiple cellular responses, including stimulation of cell migration, cell proliferation, fibrosis, vasculogenesis, and ion channel activation (12,13). Although previously implicated in CAVS pathophysiology (10,14), it has never been correlated to CAVS severity or hemodynamic progression rate. Autotaxin (ATX), which is enriched in the lipid fraction of Lp(a), is the major enzyme that catalyzes the hydrolysis of extracellular lysophospholipids to generate LysoPA (13,15,16). In the present study, the level of LysoPA was found to be higher in patients with severe AS than in those with mild AS. This finding strongly suggests that as mineralization in AV increases, the enzymatic activity of ATX increases, promoting the conversion of lysophospholipids to LysoPA. These findings are consistent with recent studies by Bouchareb et al. (14,17) and Nsaibia et al. (18), who showed that ATX together with LysoPA produced from valve interstitial cells and activated platelets promote the progression of CAVS. Further supporting the link between LysoPA and CAVS, we found that elevated LysoPA levels are also associated with faster hemodynamic progression. Zheng et al. (19) showed that stenotic patients with elevated Lp(a) levels have faster hemodynamic progression. Therefore, our data extend their finding by demonstrating that LysoPA, the end product of Lp(a) metabolism, has an important role in disease progression. The possibility of performing absolute quantification of LysoPA (a lipid) compared to Lp(a) (a protein) makes LysoPA a more robust CAVS marker. Compared to TAV stenosis, BAV stenosis is associated with increased cardiac impairment and worse survival following AV replacement (20). For the first time, we present the finding that no significant diversity in metabolome exists between these 2 populations, which suggests that underlying biochemical activity and the state of cells/tissues were similar between TAV and BAV during this disease.

Hierarchical clustering heat map depicting the expression patterns of significantly differential metabolites and lipids across different disease stages revealed clustering between the moderate and severe stages of CAVS (Figure 2). Overall, the levels of metabolites and lipids in both the moderate and severe stages were similar yet differed substantially compared to the mild stage of CAVS. This result is consistent with the hypothesis that CAVS disease progression consists of 2 different phases: an early-stage initiation phase very similar to atherosclerosis, and a later propagation phase mainly driven by mineralization (21). From our analysis, we also observed a strong association between the bile salt glycoursodeoxycholic acid and Vmax/MPG. The amounts of 2 bile salts, whose identities were further validated by theoretical fragmentation patterns (glycoursodeoxycholic acid and cholic acid), were lesser in the mild stage than in the moderate and severe stages of CAVS (Figure 2). This is an intriguing observation given that 2 recent studies, although contradicting, reported interplay between ATX-LysoPA signaling and bile salts. In the first study,

the amount of bile salt (including glycoursodeoxy-ycholic acid) exhibited a significant positive correlation with ATX activity in patients with primary biliary cholangitis disease (22). However, the second study showed that bile salt, such as tauroursodeoxycholate, noncompetitively inhibits ATX activity (23). This finding raises interesting questions about the role of bile acids in CAVS progression and calls for further investigation.

STUDY LIMITATIONS. First, although the present study examined the association between metabolomic signatures in stenotic AV leaflets and CAVS severity, the underlying biochemical mechanisms responsible for the causal relationship of these associations still are unclear. Second, apart from the ∼600 identified metabolites and lipids, approximately 3,700 reproducible peaks remain to be identified even after the database search. High-throughput analytical platforms that allow the identification and quantification of diverse metabolite and lipid classes are now available and should be pursued to gain greater insight into the tissue metabolome; however, these usually are more expensive and labor-intensive. Third, 2 LysoPA species (18:2 and 20:4 LysoPA) showed potential as biomarkers of disease progression in clinical diagnosis. Because this finding is limited by its small sample size, further investigation in an independent large cohort using plasma as the sample is needed.

CONCLUSIONS

By performing the largest reported metabolic profiling of stenotic calcified AVs in humans, we identified novel metabolites and lipids that associate with CAVS and support the role of LysoPAs in CAVS pathophysiology. The risk association of elevated levels of LysoPAs with CAVS severity is independent of traditional risk factors, including age, sex, lipid profile, glucose level, creatinine level, smoking habit, prevalence of hypertension, and presence of BAV. In addition, an elevated level of LysoPAs could select patients who are at risk for faster rate of CAVS progression. It is hoped that this novel understanding of metabolic perturbations in stenotic AVs can translate into new therapeutic interventions.

AUTHOR DISCLOSURES

ADDRESS FOR CORRESPONDENCE: Dr. Amir Ravandi, Cardiovascular Lipidomics Laboratory, St. Boniface Hospital, Albrechtsen Research Centre, 351 Tache Avenue, Winnipeg R2H 2A6, Canada. E-mail: aravandi@sbgh.mb.ca.

PERSPECTIVES

COMPETENCY IN MEDICAL KNOWLEDGE: Despite being the most prevalent valvular disease in developed countries, no medical therapies are available for CAVS. The only treatment option available is valve replacement after the patient has exhibited symptoms. Many patients are followed for many years with 2-dimensional echocardiographic diagnosis of AS before they become symptomatic. A therapeutic intervention would attenuate stenotic progression and negate the need for valvular replacement. The biggest barrier to developing therapies is the lack of detailed knowledge of the mechanisms that lead to valvular calcification and stenosis. In traditional scientific approaches, a specific pathway or cellular mechanism is targeted and its impact measured. With currently available mass spectrometric technologies, we can monitor the entire valvular metabolome without a specific target. This allows for identification of pathways directly involved in severity of disease and its progression. In the present study, we determined the most comprehensive metabolomic atlas of human aortic valve tissue at different stages of disease. This revealed that lipid molecules are the most perturbed molecules in disease progression. Specifically, LysoPA is an independent predictor of valvular stenosis and progression when measured in valvular tissue and in plasma.

TRANSLATIONAL OUTLOOK: Modulation of the LysoPA pathway has not been tested previously in a clinical setting. LysoPA is generated by the enzyme autotaxin, which resides on the Lp(a) particle. Recent antisense Lp(a) therapies have shown that they can reduce Lp(a) levels dramatically. Future studies will investigate the effect of these antisense therapies on CAVS progression.

REFERENCES

1. Nkomo VT, Gardin JM, Skelton TN, Gottdiener JS, Scott CG, Enriquez-Sarano M. Burden of valvular heart diseases: a population-based study. Lancet 2006;368:1005–11.

2. Baumgartner H, Falk V, Bax JJ, et al., ESC Scientific Document Group. 2017 ESC/EACTS Guidelines for the management of valvular heart disease. Eur Heart J 2017;38:2739–91.

3. Arsenault BJ, Boekholdt SM, Dubé MP, et al. Lipoprotein(a) levels, genotype, and incident aortic valve stenosis: a prospective Mendelian randomization study and replication in a case-control cohort. Circ Cardiovasc Genet 2014;7:304–10.

4. Kamstrup PR, Tybjaerg-Hansen A, Nordestgaard BG. Elevated lipoprotein(a) and risk of aortic valve stenosis in the general population. J Am Coll Cardiol 2014;63:470–7.

5. Schlotter F, Halu A, Goto S, et al. Spatiotemporal multi-omics mapping generates a molecular atlas of the aortic valve and reveals networks driving disease. Circulation 2018;138:377–93.

6. Patti GJ, Yanes O, Siuzdak G. Innovation: metabolomics: the apogee of the omics trilogy. Nat Rev Mol Cell Biol 2012;13:263–9.

7. Haug K, Salek RM, Conesa P, et al. Metabo-Lights—an open-access general-purpose repository for metabolomics studies and associated meta-data. Nucleic Acids Res 2013;41:D781–6.

8. Kanehisa M, Furumichi M, Tanabe M, Sato Y, Morishima K. KEGG: new perspectives on genomes, pathways, diseases and drugs. Nucleic Acids Res 2016;45:D353–61.

9. Rosato A, Tenori L, Cascante M, De Atauri Carulla PR, Martins Dos Santos VAP, Saccenti E. From correlation to causation: analysis of metabolomics data using systems biology approaches. Metabolomics 2018;14:37.

10. Torzewski M, Ravandi A, Yeang C, et al. Lipoprotein(a) associated molecules are prominent components in plasma and valve leaflets in calcific aortic valve stenosis. J Am Coll Cardiol Basic Trans Science 2017;2:229–40.

11. McGarrah RW, Crown SB, Zhang G-F, Shah H, Newgard CB. Cardiovascular metabolomics. Circ Res 2018;122:1238–58.

12. Choi JW, Herr DR, Noguchi K, et al. LPA receptors: subtypes and biological actions. Annu Rev Pharmacol Toxicol 2010;50:157–86.

13. van Meeteren LA, Moolenaar WH. Regulation and biological activities of the autotaxin-LPA axis. Prog Lipid Res 2007;46:14560.

14. Bouchareb R, Mahmut A, Nsaibia MJ, et al. Autotaxin derived from lipoprotein(a) and valve interstitial cells promotes inflammation and mineralization of the aortic valve. Circulation 2015;132:677–90.

15. Perrakis A, Moolenaar WH. Autotaxin: structure-function and signaling. J Lipid Res 2014;55:1010–8.

16. Mathieu P, Boulanger M-C. Autotaxin and lipoprotein metabolism in calcific aortic valve disease. Front Cardiovasc Med 2019;6:18.

17. Bouchareb R, Boulanger MC, Tastet L, et al. Activated platelets promote an osteogenic programme and the progression of calcific aortic valve stenosis. Eur Heart J 2019;40:1362–73.

18. Nsaibia MJ, Boulanger MC, Bouchareb R, et al. OxLDL-derived lysophosphatidic acid promotes the progression of aortic valve stenosis through a LPAR1-RhoA-NF-kappaB pathway. Cardiovasc Res 2017;113:1351–63.

19. Zheng KH, Tsimikas S, Pawade T, et al. Lipoprotein(a) and oxidized phospholipids promote valve calcification in patients with aortic stenosis. J Am Coll Cardiol 2019;73:2150–62.

20. Huntley GD, Thaden JJ, Alsidawi S, et al. Comparative study of bicuspid vs. tricuspid aortic valve stenosis. Eur Heart J Cardiovasc Imaging 2018;19:3–8.

21. Porras AM, Shanmuganayagam D, Meudt JJ, et al. Development of aortic valve disease in familial hypercholesterolemic swine: implications for elucidating disease etiology. J Am Heart Assoc 2015;4:e002254.

22. Hegade VS, Pechlivanis A, McDonald JAK, et al. Autotaxin, bile acid profile and effect of ileal bile acid transporter inhibition in primary biliary cholangitis patients with pruritus. Liver Int 2019;39:967–75.

23. Keune W-J, Hausmann J, Bolier R, et al. Steroid binding to Autotaxin links bile salts and lysophosphatidic acid signalling. Nat Commun 2016;7:11248.

KEY WORDS aortic stenosis, calcific aortic valve stenosis, lysophosphatidic acids, nontargeted metabolomics, targeted lipidomics, valvular calcification

APPENDIX For an expanded Methods section and supplemental tables and figures, please see the online version of this paper.